

## Heme bioavailability and signaling in response to stress in yeast cells

David A. Hanna<sup>1</sup>, Rebecca Hu<sup>1</sup>, Hyojung Kim<sup>1,2</sup>, Osiris Martinez-Guzman<sup>1</sup>, Matthew P. Torres<sup>2,3</sup>, and Amit R. Reddi<sup>1,3,\*</sup>

From the <sup>1</sup>School of Chemistry & Biochemistry, Georgia Institute of Technology, Atlanta, GA 30332; <sup>2</sup>School of Biological Sciences, Georgia Institute of Technology, Atlanta, GA 30332; <sup>3</sup>Parker Petit Institute for Bioengineering & Biosciences, Georgia Institute of Technology, Atlanta, GA 30332

Running title: Stress induced heme signaling

\*To whom correspondence should be addressed: Amit R. Reddi: School of Chemistry & Biochemistry, Georgia Institute of Technology, Atlanta, GA 30332; [amit.reddi@chemistry.gatech.edu](mailto:amit.reddi@chemistry.gatech.edu); Tel. (404) 385-1428.

Keywords: heme, heavy metals, lead, Hap1, heme sensors, labile heme pool, cell stress, yeast, xenobiotic

### ABSTRACT

Protoheme (hereafter referred to as heme) is an essential cellular cofactor and signaling molecule that is also potentially cytotoxic. To mitigate heme toxicity, heme synthesis and degradation are tightly coupled to heme utilization in order to limit the intracellular concentration of “free” heme. Such a model, however, would suggest that a readily accessible steady-state, bioavailable labile heme (LH) pool is not required for supporting heme-dependent processes. Using the yeast *Saccharomyces cerevisiae* as a model and fluorescent heme sensors, site-specific heme chelators, and molecular genetic approaches, we found here that (1) yeast cells preferentially use LH in heme-depleted conditions; (2) sequestration of cytosolic LH suppresses heme signaling; and (3) lead (Pb<sup>2+</sup>) stress contributes to a decrease in total heme, but an increase in LH, which correlates with increased heme signaling. We also observed that the proteasome is involved in the regulation of the labile heme pool and that loss of proteasomal activity sensitizes cells to Pb<sup>2+</sup> effects on heme homeostasis. Overall, these findings suggest an important role for LH in supporting heme-dependent functions in yeast physiology.

Protoheme (iron protoporphyrin IX or heme *b*) is an essential cofactor and signaling molecule that is also potentially cytotoxic (1-4). The molecules and mechanisms cells employ to utilize protoheme, while mitigating its inherent

toxicity, are complex and poorly understood, especially during stress (1,2). Cells manage protoheme, which is hereafter referred to as heme, by controlling both its total concentration and bioavailability (1,2). Heme concentration is primarily governed by the relative rates of heme synthesis and degradation, which are well-understood processes (1,2). Indeed, all the enzymes involved in eukaryotic heme synthesis and degradation have been structurally characterized to atomic resolution and the mechanisms of action have been largely delineated (1-4).

On the other hand, the factors that control heme bioavailability are poorly understood (1,2). Bioavailable heme can be operationally defined as a pool of chelatable, kinetically labile heme that can readily exchange between biomolecules and is accessible for heme-dependent processes. The identity of factors that buffer and traffic labile heme (LH) and the mechanisms employed to mobilize it for utilization are largely unknown (1,2).

In order to mitigate heme toxicity, it is generally thought that heme is made on demand, *i.e.* heme synthesis and utilization are tightly coupled, and heme in excess of that required for metabolism is degraded (4-6). As a consequence, it is unclear what role, if any, steady-state LH plays in supporting heme dependent functions. Using genetically encoded ratiometric fluorescent heme sensors to probe LH and heme homeostatic mechanisms, we have previously demonstrated the

existence of a highly dynamic steady-state pool of LH in the cytosol, spanning 20-40 nM, and identified new heme trafficking factors, *e.g.* glyceraldehyde phosphate dehydrogenation (GAPDH), and signaling molecules that mobilize LH, *e.g.* nitric oxide (NO) (7). However, the physiological importance of LH remained unclear.

In the current work, using *Saccharomyces cerevisiae* as a model eukaryote and heme sensors and chelating agents, we establish the functional importance of LH in regulating heme signaling, demonstrate that LH is preferentially consumed when cells become heme depleted, and discovered that certain xenobiotics, *e.g.* lead ions ( $\text{Pb}^{2+}$ ), can, rather paradoxically, both deplete total cellular heme, primarily through its inhibition of heme synthesis, and increase labile bioavailable heme. We further find that the proteasome is involved in the regulation of labile heme and its response to  $\text{Pb}^{2+}$  stress. In total, our results establish a functional role for LH, indicate that total and labile heme pools can be decoupled in response to certain stressors, and provide evidence for heme-based signaling in response to heavy metal stress.

## Results

### *Sequestering labile heme impacts heme signaling*

We first sought to determine if cytosolic LH serves a functional role in heme signaling. Towards this end, we developed an approach to sequester LH and probe its effects on the heme-regulated transcription factor Hap1 (8-11). In order to chelate cytosolic LH, we induced the expression of a high affinity hemoprotein, cytochrome  $b_{562}$  (Cyt  $b_{562}$ ) (12-16), using a galactose (GAL)-inducible promoter (pGAL) (17). Cyt  $b_{562}$  binds ferric heme at pH 7.0 with a dissociation constant ( $K_D^{\text{III}}$ ) of 10 nM (16). Given the reduction potential ( $E_M$ ) of heme-Cyt  $b_{562}$ , +200 mV vs. NHE at pH 7.0 (18), and the  $E_M$  of free heme, -38 mV vs. NHE (19,20), one can estimate the ferrous heme dissociation constant ( $K_D^{\text{II}}$ ) to be ~1 pM by completing a thermodynamic cycle (19).

First, we confirmed that Cyt  $b_{562}$  overexpression could sequester heme by measuring changes in LH with the genetically encoded ratiometric fluorescent heme sensor, HS1-M7A (7). HS1 is a tri-domain fusion protein consisting of a heme-binding domain, the His/Met coordinating 4- $\alpha$ -helical bundle hemoprotein

cytochrome  $b_{562}$  (Cyt  $b_{562}$ ), fused to a pair of fluorescent proteins, eGFP and mKATE2, that exhibit heme-sensitive and -insensitive fluorescence, respectively (7) (**Fig. 1A**). Heme binding to the Cyt  $b_{562}$  domain results in the quenching of eGFP fluorescence via resonance energy transfer but has little effect on mKATE2 fluorescence (7). Thus, the ratio of eGFP fluorescence (ex: 488 nm, em: 510 nm) to mKATE2 fluorescence (ex: 588 nm, em: 620 nm) provides a readout of cellular heme independently of sensor concentration, with the eGFP/mKATE2 ratio inversely correlating with heme binding to the sensor (7). The high affinity of HS1 for ferric and ferrous heme,  $K_D^{\text{III}} = 10$  nM and  $K_D^{\text{II}} < 1$  nM at pH 7.0, renders it fully saturated with heme in WT cells (7). On the other hand, a variant of HS1, HS1-M7A, in which the heme coordinating Met ligand is mutated to Ala, exhibits ferrous and ferric affinities of  $K_D^{\text{II}} = 25$  nM and  $K_D^{\text{III}} = 2$   $\mu\text{M}$  at pH 7.0 and is 20-50% bound in the yeast cytosol (7). The observed sensor eGFP/mKATE2 fluorescence ratio ( $R_{\text{expt}}$ ) can be used to determine the fractional heme saturation of the sensor and the concentration of LH, assuming a 1:1 heme:sensor binding model and previously established sensor calibration protocols that involve determining the sensor ratio when the sensor is 100% ( $R_{\text{max}}$ ) and 0% ( $R_{\text{min}}$ ) bound to heme (see **Method Details**) (7). Notably, heme binding to the sensor is reversible and expression of the heme sensor in cells does not itself perturb heme homeostasis or otherwise affect viability (7).

Wild type (WT) cells expressing heme sensor HS1-M7A and GAL-inducible Cyt  $b_{562}$  (pGAL- Cyt  $b_{562}$ ) were cultured in 2% raffinose (RAF) with or without 0.1% GAL for 16 hours. As demonstrated in **Fig. 1B**, induction with GAL results in an increase in the eGFP/mKATE2 fluorescence ratio, from 1.90 (.09) to 2.82 (.04), consistent with less heme binding to the sensor and diminished LH. By comparison, cells expressing an empty pGAL vector (EV) or that are heme depleted with the heme biosynthetic inhibitor, succinylacetone (SA) (7,21,22), are unaffected by induction of Cyt  $b_{562}$ . Using the aforementioned sensor calibration protocols, which are described in detail in the **Method Details** section, the induction of Cyt  $b_{562}$  results in a decrease in the fractional saturation of the heme

sensor from ~60% to ~35% heme bound, which corresponds to a change in LH from 35 to 14 nM.

Having established that LH can be sequestered by over-expression of Cyt *b*<sub>562</sub>, we next sought to determine if this would impact the activity of the heme regulated transcription factor Hap1 (8-11). Heme binding to Hap1 alters its ability to promote or repress transcription of a number of target genes, including *CYC1*, which Hap1 positively regulates (7-11). In order to probe Hap1 activity, we used a transcriptional reporter that employs the promoter of a Hap1 target gene, *pCYC1*, driving the expression of enhanced green fluorescent protein (eGFP) (7). As demonstrated in **Fig. 1C**, not only does heme depletion with SA decrease eGFP fluorescence, as expected, Cyt *b*<sub>562</sub> induction with GAL also results in a decrease in eGFP fluorescence, both of which are consistent with reduced heme binding to Hap1 and diminished transcriptional activation of *CYC1*. Altogether, our results strongly suggest that over-expression of Cyt *b*<sub>562</sub> can sequester LH and this results in diminished heme signaling and Hap1 activity.

### ***LH is preferentially consumed relative to total heme during heme depletion***

We next sought to determine if LH is consumed preferentially relative to total heme during conditions of heme deficiency in order to ascertain if LH is mobilized for heme dependent functions when cells are confronted with defects in heme synthesis. Towards this end, we titrated the heme biosynthetic inhibitor succinylacetone (SA) in WT cells expressing the high affinity heme sensor, HS1, or the medium affinity sensor, HS1-M7A, and measured total and labile heme (**Fig. 2**). Titration of SA over a broad concentration range, up to 500  $\mu$ M, results in the depletion of both total (**Fig. 2C**) and labile heme (**Fig. 2A and 2B**) as expected. However, most interestingly, LH is more sensitive than total heme to SA-mediated heme depletion (**Fig. 2**). When total heme is only modestly depleted by 25% using a relatively low 25  $\mu$ M dose of SA (**Fig. 2C**), there is a much larger diminution of LH as measured by HS1-M7A and HS1 (**Fig. 2A and 2B**); heme loading of the medium affinity sensor, HS1-M7A, shifts from ~26% bound to ~0% bound, and the high affinity sensor, HS1, shifts in heme loading from ~100% bound to ~60% bound. In terms of LH

concentration, based on the ferrous heme dissociation constants of HS1-M7A,  $K_D^{\text{II}} = 25$  nM (7), and HS1, assumed to be  $K_D^{\text{II}} \sim 1$  pM based on the estimated  $K_D^{\text{II}}$  for Cyt *b*<sub>562</sub>, we would estimate LH decreases from ~10 nM to < 1 nM (likely ~2 pM based on the predicted  $K_D^{\text{II}}$  for HS1) in response to an SA concentration that modestly depletes total heme by 25%. Taken together, these data strongly suggest that heme deficiency mobilizes labile heme to non-exchangeable, and likely higher affinity and/or buried, heme-binding sites.

### ***Pb<sup>2+</sup> depletes total heme but increases labile heme and heme mediated signaling***

A number of xenobiotics and environmental toxins negatively impact heme homeostasis (23), including N-methylprotoporphyrins (24,25), certain alkylating agents, *e.g.* 2-Allyl-2- isopropylacetamide (26), tetrachlorodibenzo-p-dioxin and various polyhalogenated biphenyls (27,28), and heavy metals (29-34). Pb<sup>2+</sup>, in particular, is a major public health concern given the ubiquity of Pb<sup>2+</sup>-based paints, piping, and munitions (34). Among other targets, Pb<sup>2+</sup> is well known to inhibit heme biosynthetic enzymes aminolevulinic acid (ALA) dehydratase (ALAD) and ferrochelatase (FECH), resulting in defects in heme synthesis, which in-turn leads to anemia, cognitive decline, and other health problems (34). Further, Pb<sup>2+</sup> and other heavy metals are known to induce HO (35,36), which may also contribute to decreased heme levels. However, while much is known about the role of Pb<sup>2+</sup> in impacting heme synthesis and degradation, virtually nothing is known about the effects of Pb<sup>2+</sup> on bioavailable labile heme. Given our findings that LH is important for maintaining heme signaling to Hap1 and is preferentially consumed relative to total heme during heme deficiency, we sought to determine the effects of Pb<sup>2+</sup> on LH and heme-based signaling. Towards this end, we established a yeast model of Pb<sup>2+</sup> toxicity and probed the effects of Pb<sup>2+</sup> on total heme, LH, and heme signaling.

Due to the insolubility of Pb(NO<sub>3</sub>)<sub>2</sub> in standard yeast growth medias, we employed a Pb<sup>2+</sup> toxicity model similar to what was previously described in which yeast cells are subjected to an acute 3 hour exposure to varying concentrations of Pb<sup>2+</sup> in 10 mM 2-(N-morpholino)ethanesulfonic

acid (MES), pH = 6.0 buffer, a media in which  $\text{Pb}(\text{NO}_3)_2$  is soluble and  $\text{Pb}^{2+}$  is not complexed by the buffer (37). Following  $\text{Pb}^{2+}$  exposure, cells are washed and allowed to recover for 4 hours in an appropriate synthetic complete (SC) drop-out media prior to subsequent analyses. Cell viability is measured by diluting cells into SC media after the recovery period and monitoring growth for 20 hours. Cell viability as measured by outgrowth is virtually identical to viability measurements using FUN-1, a fluorescent dye that exhibits red punctate emission in the vacuoles of metabolically active live cells and diffuse green cytosolic emission in dead cells (**Fig. S1A-C**) (37). As shown in **Fig. 3A**, yeast viability decreases with increasing  $[\text{Pb}^{2+}]$ . The concentration of  $\text{Pb}^{2+}$  that inhibits growth by 50%, lethal dose-50 ( $\text{LD}_{50}$ ), varied between 25 and 500  $\mu\text{M}$  over the course of our studies with different batches of media for reasons that are not completely understood. As a consequence, all of our analyses were done at the  $\text{Pb}^{2+}$   $\text{LD}_{50}$  dose and not necessarily at a constant  $\text{Pb}^{2+}$  concentration.

At the  $\text{Pb}^{2+}$   $\text{LD}_{50}$  dose, elemental analysis using total reflection X-ray fluorescence (TXRF) spectroscopy confirms a significant enrichment of  $\text{Pb}^{2+}$  in yeast cells (**Fig. 3B**). In addition, a host of other bio-elements are impacted as a consequence of  $\text{Pb}^{2+}$  toxicity; P, S, K, Fe, and Zn are diminished, whereas Ca and Cu are increased (**Fig. S2**). These effects are consistent with prior studies in a number of organisms and cell types demonstrating the impact of  $\text{Pb}^{2+}$  on various aspects of metal (37-42), phosphate (43,44), and sulfur homeostasis (45-47).

Interestingly, while total heme is depleted due to  $\text{Pb}^{2+}$  exposure, as expected due to its known effects on inhibiting heme synthesis (34) and up-regulating heme degradation (35,36), LH is completely maintained, and in fact, increases by 2-fold (**Fig. 3C**). In striking contrast, a dose of SA that depletes total heme to a similar degree as  $\text{Pb}^{2+}$  treatment attenuates both LH and total heme (**Fig. 3C**). Titration of  $\text{Pb}^{2+}$  over a broad concentration range indicates a dose dependent increase in LH (**Fig. 4A**), decrease in total heme (**Fig. 4B**), and decrease in cell viability (**Fig. 4C**). The  $\text{Pb}^{2+}$ -dependent depletion of total heme and increase in LH primarily occurs after the recovery period in SC media; measurement of total heme and LH after the 3 hour  $\text{Pb}^{2+}$  exposure in MES buffer has

minimal effects on LH (**Fig. 4D**) and total heme (**Fig. 4E**) relative to cells allowed to recover in SC media (**Figs. 4A and 4B**). The changes in HS1-M7A sensor ratio are not due to artifacts associated with  $\text{Pb}^{2+}$ -dependent changes in sensor expression given that the emission of mKATE2, the heme-insensitive fluorophore, is constant over a wide-range of  $\text{Pb}^{2+}$  doses (**Fig. S3A**). Furthermore, a variant of HS1 that cannot bind heme, HS1-M7A, H102A, which has the Met and His heme coordinating residues mutated to Ala, does not exhibit  $\text{Pb}^{2+}$ -dependent changes in fluorescence ratio (**Fig. S3B**). Altogether, these data indicate that the total and labile heme pools can be acted upon independently of each other in response to stress and metabolically active cells are required for the observed changes in  $\text{Pb}^{2+}$ -dependent LH and total heme.

We next addressed if the increase in LH in response to  $\text{Pb}^{2+}$  translates to changes in heme signaling. Towards this end, we measured Hap1 activity using the *pCYC1-eGFP* transcriptional reporter in cells conditioned with the  $\text{LD}_{50}$  dose of  $\text{Pb}^{2+}$ . In order to account for the effects of  $\text{Pb}^{2+}$  on eGFP expression independently of Hap1 activation, we also expressed eGFP under control of the *GPD* promoter (*pGPD*), which is not a transcriptional target of Hap1. As shown in **Fig. 3D**, exposure to  $\text{Pb}^{2+}$  results in a ~33% decrease in the eGFP fluorescence of the Hap1 reporter while SA exposure results in a 6-fold decrease, despite a similar depletion in total heme.

Given that  $\text{Pb}^{2+}$  also affects eGFP fluorescence independently of Hap1, as evidenced by a ~60% decrease in fluorescence of parallel cultures harboring the *pGPD-eGFP* construct, we normalized the fluorescence from *pCYC1* driven expression of eGFP to the fluorescence from *pGPD* driven expression of eGFP, giving a *pCYC1/pGPD* ratio. Exposure to  $\text{Pb}^{2+}$  results in a nearly 2-fold increase, from .16 to .26, in the *pCYC1/pGPD* ratio of eGFP fluorescence, an indicator of Hap1/*pCYC1* specific activation. In striking contrast, cells conditioned with a dose of SA that results in a similar concentration of intracellular heme as the  $\text{LD}_{50}$  dose of  $\text{Pb}^{2+}$  exhibits a nearly ~10-fold decrease in the *pCYC1/pGPD* ratio of eGFP fluorescence, with a nearly 10-fold decrease in fluorescence of the *pCYC1-eGFP* construct and minimal perturbation to fluorescence from the *pGPD-eGFP* construct.



Taken together, at minimum, these results suggest that, in response to  $Pb^{2+}$  toxicity, Hap1 activity is largely maintained, despite a > 10-fold decrease in total heme. At maximum, these results suggest that “heme-specific” Hap1 activity, as recorded from the pCYC1/pGPD ratio, actually increases in response to  $Pb^{2+}$  stress. The maintenance of or increase in Hap1 activity, depending on the interpretation of the data, is presumably due to the  $Pb^{2+}$ -induced increase in LH.

***$Pb^{2+}$ -mediated heme depletion is largely due to a block in heme synthesis.***

We next sought to determine the mechanism by which intracellular heme is depleted in response to  $Pb^{2+}$  toxicity. The intracellular concentration of heme is governed by the relative rates of heme synthesis and degradation or export. In order to parse apart the effects of  $Pb^{2+}$  on these opposing processes, we tested the effects of  $Pb^{2+}$  on cells that had a defect in the ability to synthesize heme. First, we determined that  $Pb^{2+}$ -dependent heme depletion occurs within the first 1.5 hours of the 4-hour recovery period in SC media (**Fig. 5A**, 0  $\mu$ M SA). Second, we found that in cells that had a defect in heme synthesis due to conditioning with 500  $\mu$ M SA,  $Pb^{2+}$  had an attenuated effect on the loss of total heme. For instance, after 2.7 hours, cells that could biosynthesize heme (**Fig. 5A**, 0  $\mu$ M SA) exhibited a 2-fold and 6-fold decrease in total heme when treated with 125 and 250  $\mu$ M  $Pb^{2+}$ , respectively. On the other hand, in cells with ablated heme biosynthesis (**Fig. 5A**, 500  $\mu$ M SA), both 125 and 250  $\mu$ M  $Pb^{2+}$  resulted in a relatively modest ~30% decrease in total heme. The diminished effect of  $Pb^{2+}$  on total heme in cells conditioned with the heme biosynthetic inhibitor SA suggested that  $Pb^{2+}$  depletes total heme by largely suppressing heme biosynthesis.

We next sought to further validate the observation that  $Pb^{2+}$  depletes heme by primarily affecting heme synthesis and not heme degradation or export. Towards this end, we utilized a *hem1* $\Delta$  strain, which lacks the 1<sup>st</sup> enzyme in the heme synthesis pathway, ALA synthase (ALAS), to test the effects of  $Pb^{2+}$  on the degradation of mitochondrially-derived *de novo* synthesized heme or exogenously supplied heme. *hem1* $\Delta$  cells can only acquire heme by stimulating

mitochondrial heme synthesis via supplementation with ALA, the product of ALAS, or by heme uptake via hemin supplementation. We supplemented *hem1* $\Delta$  cells with ALA or heme during a 16-hour pre-culture in SCE media, subjected them to  $Pb^{2+}$  exposure in MES buffer for 3 hours, followed by a 4-hour recovery in SCE media, and then analyzed total heme (**Fig. 5B**). WT and *hem1* $\Delta$  cells supplemented with ALA in both the pre-culture and during the recovery accumulated similar amounts of intracellular heme, experienced a  $Pb^{2+}$ -dependent depletion of total heme (**Fig. 5B**, black and green columns) and exhibited > 80% heme-loading of the high affinity heme sensor HS1 (**Fig. 5C**, black and green columns). *hem1* $\Delta$  cells treated with ALA only during the pre-culture, but not during the recovery, also exhibited a  $Pb^{2+}$ -dependent attenuation in intracellular heme (**Fig. 5B**, red columns). However, the total amount of heme was ~5-fold lower (**Fig. 5B**, red columns) and the heme-loading of HS1 was considerably reduced, ~10% bound, compared to *hem1* $\Delta$  cells supplemented with ALA in both the pre-culture and the recovery media (**Fig. 5C**, red columns), presumably due to the fact that ALA was limiting since it is not supplied during the recovery phase. In striking contrast to ALA supplementation, *hem1* $\Delta$  cells supplemented with exogenous heme during the pre-culture, which contributed to a 2-fold increase in intracellular heme relative to ALA supplemented *hem1* $\Delta$  cells, did not exhibit the  $Pb^{2+}$ -dependent depletion of heme (**Fig. 5B**, yellow columns). Exogenously supplied heme is still available to bind HS1, and in fact, its fractional saturation is similar to ALA treated cells after normalizing for the change in total intracellular heme concentration (**Fig. 5C**, yellow columns). The observation that  $Pb^{2+}$  depletes endogenously synthesized heme and not exogenously supplied heme strongly suggests that  $Pb^{2+}$  primarily inhibits heme synthesis, with minor effects on heme degradation.

Given that heme synthesis is  $O_2$ -dependent and our results that  $Pb^{2+}$  largely inhibits heme synthesis, we next sought to test our prediction that  $Pb^{2+}$  should have minimal impact on total heme in the absence of  $O_2$ . To test the  $O_2$  dependence of  $Pb^{2+}$ -induced heme depletion, we subjected aerobically grown cells to  $Pb^{2+}$  exposure in MES buffer in an anoxic or normoxic

environment, followed by recovery in anoxic or normoxic culture conditions and measurement of total heme, LH, and  $\text{Pb}^{2+}$  toxicity (**Fig. 6**). Quite strikingly, despite accumulating similar levels of  $\text{Pb}^{2+}$  between normoxic and anoxic  $\text{Pb}^{2+}$ -exposures (**Fig. S4**), in the absence of  $\text{O}_2$ , cells do not exhibit  $\text{Pb}^{2+}$ -dependent heme depletion (**Fig. 6A**). On the other hand, the increase in LH in response to  $\text{Pb}^{2+}$  is similar between both normoxic and anoxic  $\text{Pb}^{2+}$  exposures (**Fig. 6B**). Notably,  $\text{Pb}^{2+}$ -mediated cell toxicity is entirely  $\text{O}_2$ -dependent given that viability is not affected in anoxic cultures (**Fig. 6C**). Taken together, our data suggest that  $\text{Pb}^{2+}$ -induced depletion of total heme only occurs in cells that are synthesizing heme *de novo*, further supporting the notion that  $\text{Pb}^{2+}$  largely inhibits heme synthesis.

We next sought to determine if a block in heme degradation or export could preserve total heme in the face of  $\text{Pb}^{2+}$  toxicity and affect labile heme. One established mechanism of heme degradation is via heme oxygenase (HO), an enzyme that oxidatively degrades heme into bilirubin, carbon monoxide (CO), and ferrous iron ( $\text{Fe}^{2+}$ ) (36). In order to test the role of HO in  $\text{Pb}^{2+}$ -dependent heme depletion, we compared WT and *hmx1* $\Delta$  cells, which lacks heme oxygenase 1 (48,49), for  $\text{Pb}^{2+}$ -dependent heme depletion. As shown in **Fig. 7A**, in the absence of  $\text{Pb}^{2+}$ , *hmx1* $\Delta$  cells exhibit a ~25% increase in total heme, consistent with prior studies in yeast and the known role of Hmx1 in heme degradation (48). However, both WT and *hmx1* $\Delta$  cells exhibit the  $\text{Pb}^{2+}$ -induced depletion of heme to similar degrees, indicating HO does not play a role in the loss of heme during  $\text{Pb}^{2+}$  toxicity. Both WT and *hmx1* $\Delta$  cells exhibited a  $\text{Pb}^{2+}$ -dependent increase in LH (**Fig. 7B**). For reasons that are not entirely clear at this time, *hmx1* $\Delta$  cells appeared to be more resistant to  $\text{Pb}^{2+}$  toxicity (**Fig. 7C**). In contrast, prior work has demonstrated that Hmx1p confers resistance to various oxidative insults, including  $\text{H}_2\text{O}_2$ , diamide, and menadione (49), presumably due to released CO, bilirubin, and biliverdin.

An alternative mechanism for cellular heme depletion is heme export. Many metazoans express heme exporters, *e.g.* FLVCR1, to aid in heme detoxification. *Saccharomyces cerevisiae* expresses a porphyrin-heme exchanger, *PUG1*, which uptakes protoporphyrin IX and expels heme (50). In order to test the role of heme export via

*Pug1* during  $\text{Pb}^{2+}$  toxicity, we determined the extent to which heme is depleted in WT and *pug1* $\Delta$  cells exposed to increasing doses of  $\text{Pb}^{2+}$ . As with *hmx1* $\Delta$  cells, *pug1* $\Delta$  cells exhibit a similar degree of  $\text{Pb}^{2+}$ -induced heme depletion as WT cells (**Fig. 7D**), indicating *Pug1* does not affect the loss of heme during  $\text{Pb}^{2+}$  toxicity. Both WT and *pug1* $\Delta$  cells exhibit an increase in LH in response to  $\text{Pb}^{2+}$  (**Fig. 7E**) and similar sensitivities to  $\text{Pb}^{2+}$  toxicity (**Fig. 7F**).

Altogether, our data indicate that: **a.**  $\text{Pb}^{2+}$  depletes total heme primarily through its ability to inhibit heme synthesis and **b.** heme degradation and export pathways do not affect  $\text{Pb}^{2+}$ -dependent changes in total and labile heme.

### ***Pb<sup>2+</sup>-dependent increases in labile heme correlate with protein degradation.***

Most heme is associated with non-exchangeable binding sites in high affinity hemoproteins. As such, we predicted that the increase in labile heme in response to  $\text{Pb}^{2+}$  may be associated with the degradation of hemoproteins and the release of heme into the labile heme pool. To test this hypothesis, we conducted 1-D PAGE analysis of cells conditioned with and without  $\text{Pb}^{2+}$  at the  $\text{LD}_{50}$  dose immediately after the 3-hour exposure to  $\text{Pb}^{2+}$  in MES buffer and after the 4-hour recovery phase (**Fig. 8A**). We found that immediately following exposure to  $\text{Pb}^{2+}$ , protein expression is unaffected, whereas after the 4-hour recovery, a number of proteins are degraded (**Fig. 8A**). The diminished protein expression during the recovery phase correlates with when we observe increased LH, suggesting protein turnover and an increase in LH are linked. Notably, using tandem mass spectrometry, we found that GAPDH, a component of the LH buffer (7), is retained during  $\text{Pb}^{2+}$  exposure (**Fig. 8A and 8B and Table S2**). Another glycolytic protein, enolase, is also maintained during  $\text{Pb}^{2+}$  exposure. On the other hand,  $\text{Pb}^{2+}$  has the capacity to degrade high affinity hemoproteins. Ctt1, which is a heme containing catalase enzyme, is degraded in a  $\text{Pb}^{2+}$ -dependent manner (**Fig. 8B**). Altogether, our data is consistent with a model in which  $\text{Pb}^{2+}$  induced degradation of hemoproteins releases heme that contributes to the LH pool.

In order to test the hypothesis that  $\text{Pb}^{2+}$ -dependent protein turnover releases heme from hemoproteins and increases LH, we assayed  $\text{Pb}^{2+}$ -

dependent changes in LH in yeast mutants defective in various protein degradation pathways, including vacuolar, autophagic, and proteasomal degradation. We found that a proteasome mutant, *rpn10Δ* (51), exhibited  $Pb^{2+}$  dependent and independent changes in LH (**Fig. 8C**), whereas mutants defective in vacuolar, *pep4Δ* (52), (**Fig. 8D**) or autophagic, *atg1Δ* (53), (**Fig. 8C**), pathways did not have altered LH. Under non-stressed conditions, WT cells exhibited a LH concentration of  $\sim 5$  nM, corresponding to an HS1-M7A fractional saturation of 17%. On the other hand, HS1-M7A was  $\sim 0\%$  bound to heme when expressed in *rpn10Δ* cells, which corresponds to an LH concentration of  $< 1$  nM. However,  $Pb^{2+}$  induced a greater increase in LH (**Fig. 8C**) and decrease in total heme (**Fig. 8E**) in *rpn10Δ* cells relative to WT. Moreover, the growth of *rpn10Δ* cells were more sensitive to  $Pb^{2+}$  toxicity than WT (**Fig. 8F**). In total, these results indicate that the proteasome positively regulates LH and loss of proteasomal function sensitizes cells to  $Pb^{2+}$ -dependent effects on heme homeostasis.

## Discussion

Heme synthesis and degradation is tightly coordinated so as to minimize the accumulation of potentially cytotoxic "free" or labile heme (LH) (4-6). As a consequence, the concentration and physiological role of LH in biology has been controversial (1,2). While estimates for the concentration of LH across various cell types have spanned sub-pM to  $\mu$ M quantities (1,2,5,54,55), the use of genetically encoded heme sensors in yeast and various non-erythroid human cells lines have established a consensus range for cytosolic LH that spans 10-100 nM, representing up to 10% of the total heme concentration (7,56). However, few studies have directly probed the contribution of steady-state LH as a heme source for hemoproteins and heme signaling. Herein, we established a functional role for LH in regulating heme signaling and demonstrated that LH is preferentially consumed relative to total heme when cells become heme depleted.

We find that modestly depleting total heme by 25% with succinylacetone, an inhibitor of the second enzyme in the heme biosynthetic pathway, ALAD, results in a much larger perturbation to LH, depleting it more than 10-fold,

from 10 nM to  $< 1$  nM, possibly as low as  $\sim 2$  pM (**Fig. 2**). The sensitivity of the LH pool towards heme depletion relative to total heme is an indication that LH is mobilized to support heme-dependent processes when cells are confronted with diminished heme synthesis. In other words, LH re-equilibrates with other high-affinity and/or poorly exchangeable heme binding sites that may become vacant when heme is depleted. These results are consistent with prior pulse-chase experiments that utilized radiolabelled ALA and/or heme sources to demonstrate that P450 enzymes equilibrate with LH (23). Altogether, these observations may have significant implications for conceptualizing new heme-based therapies for porphyrias, a family of inherited disorders associated with defects in heme biosynthesis. For instance, treatment methods designed to increase LH via supplementation with appropriate heme complexes may form the basis for alleviating the symptoms of heme scarcity (57).

In order to address the role of LH on heme dependent functions, we induced a site-specific heme chelator in the cytosol via the over-expression of Cyt *b*<sub>562</sub> and assessed its effect on heme signaling through the yeast heme regulated transcription factor Hap1 (**Fig. 1**). We found that sequestration of LH inhibited Hap1 activity, demonstrating that LH can control heme-signaling processes. Importantly, these results indicate that increasing heme synthesis, a metabolically demanding process, is not the only means to activate heme signaling, as was previously suggested for activation of Hap1 (10,58) and metabolic cycling in yeast (59,60), as well as heme regulation of the circadian clock through the nuclear receptors, Rev-erb- $\alpha$  and Rev-erb- $\beta$ , in mammals (61).

In order to understand the relationship between total heme, LH, and heme signaling during adaptation to cellular stress, we subjected yeast cells to an environmentally-relevant toxicant well known to affect heme homeostasis,  $Pb^{2+}$  (34). In yeast,  $Pb^{2+}$  toxicity suppresses metabolic activity and proliferation through a mechanism that requires new protein synthesis (37). In addition, mitochondria are a major target of  $Pb^{2+}$  toxicity and are the source of  $Pb^{2+}$ -induced reactive oxygen species production (ROS) (62). Heavy metal sequestration by vacuoles and

binding to glutathione and metallothioneins are important detoxification pathways for  $\text{Pb}^{2+}$  (63).

A number of previously established yeast models for  $\text{Pb}^{2+}$  toxicity employ exposures spanning 0.1 – 10 mM, which is high relative to the 240 nM  $[\text{Pb}^{2+}]$  threshold in patient blood samples used to initiate public health actions (64), the 1 – 5  $\mu\text{M}$  blood  $[\text{Pb}^{2+}]$  associated with inhibition of heme biosynthesis in humans (65,66), or the 0.1 – 250  $\mu\text{M}$   $[\text{Pb}^{2+}]$  used in mammalian cell culture models of  $\text{Pb}^{2+}$  toxicity (67,68). However, it is important to note that the biochemical features of  $\text{Pb}^{2+}$  toxicity at these high concentrations in yeast phenocopy many of the hallmarks of  $\text{Pb}^{2+}$  toxicity in mammalian cell lines at lower concentrations (37,62,63,69-71), including inhibition of heme synthesis (current work). The higher  $\text{Pb}^{2+}$  exposure concentrations required for yeast may reflect differences in  $\text{Pb}^{2+}$  uptake, efflux, or intracellular bioavailability.

While  $\text{Pb}^{2+}$  has the capacity to deplete cellular heme through its ability to inhibit two enzymes in the heme biosynthetic pathway, ALAD, also the target of SA, and FECH, and up-regulate the expression of the heme-degrading enzyme HO (34-36), we found that, in yeast,  $\text{Pb}^{2+}$  significantly attenuates total heme primarily due to the inhibition of heme synthesis (**Figs. 5 and 6**). However, rather surprisingly and paradoxically, we found that  $\text{Pb}^{2+}$  significantly increases LH (**Fig. 3C**). Given our previous findings that thiol-specific alkylating agents impact the NO-mediated mobilization of LH (7) and the well documented interactions between  $\text{Pb}^{2+}$  and cysteine residues (72), we propose that  $\text{Pb}^{2+}$  may liberate heme in cells from certain thiol containing heme binding sites. Alternatively, since  $\text{Pb}^{2+}$  induces the degradation of a large fraction of the proteome, the increase in LH could simply be a result of heme that is released from hemoproteins that are being turned-over. Consistent with this model, we found that a mutant that has a defect in proteasomal function, *rpn10 $\Delta$* , has less LH than WT cells (**Fig. 8C**). However, it is unclear why *rpn10 $\Delta$*  cells exhibit a greater magnitude increase in LH (**Fig. 8C**) and decrease in total heme (**Fig. 8E**) in response to  $\text{Pb}^{2+}$  stress. One explanation that could account for the former is that  $\text{Pb}^{2+}$  is directly or indirectly inducing the release of heme from a hemoprotein target that is stabilized due to the attenuation in proteasome function in *rpn10 $\Delta$*  cells.

Given that previous studies have demonstrated that  $\text{Pb}^{2+}$  positively regulates the proteasome (73) and heme and ALAD act as negative regulators of the proteasome (74,75), there is a complex mosaic of competing effects that might account for the  $\text{Pb}^{2+}$ -dependent changes in heme homeostasis in WT and *rpn10 $\Delta$*  cells. We are currently elucidating the molecular mechanisms underlying heme regulation of LH and the proteasome.

The  $\text{Pb}^{2+}$ -induced increase in LH seems to impact heme signaling via Hap1 (**Fig. 3D**). Indeed, despite the attenuation in total heme concentration due to  $\text{Pb}^{2+}$  toxicity (**Fig. 3C**), we still observe a level of Hap1 activity that is much greater relative to SA-mediated heme depletion (**Fig. 3D**), which attenuates both LH and total heme (**Fig. 3C**).

The observation of an increased LH pool in response to  $\text{Pb}^{2+}$  may have implications for the pathology of  $\text{Pb}^{2+}$  toxicity. For instance, the increase in LH in response to  $\text{Pb}^{2+}$  may contribute to a cytotoxic heme pool (5,6) that leads to the oxidative stress associated with  $\text{Pb}^{2+}$  toxicity (76,77). Alternatively, given that there are a number of heme regulated transcription factors, kinases, and ion channels (1,2), the increase in LH in response to  $\text{Pb}^{2+}$  may be required to activate heme-based signaling pathways important for adaptation to heavy metal stress. The specific physiological consequences of increased LH in response to  $\text{Pb}^{2+}$  stress remains to be fleshed out.

Altogether, our studies demonstrate the functional importance of LH in heme utilization, especially during stress associated with heme depletion and  $\text{Pb}^{2+}$  toxicity. Our future work will involve probing the specific mechanisms by which LH can be coupled to heme utilization, as well as the mechanisms underlying the  $\text{Pb}^{2+}$  mediated increase in LH and the physiological consequences of this action.

## Experimental procedures

### Yeast strains, transformations, and growth conditions

*S. cerevisiae* strains used in this study were derived from BY4741 (MATa, *his3 $\Delta$ 1*, *leu2 $\Delta$ 0*, *met15 $\Delta$ 0*, *ura3 $\Delta$ 0*). *pug1::KANMX4*, *hmx1::KANMX4*, *cta1::KANMX4*, and *ctt1::KANMX4* strains were obtained from the yeast gene deletion collection (Thermo Fisher Scientific) and the *hem1::HIS3* strain was described previously (7). Yeast transformations



were performed by the lithium acetate procedure (78). Strains were maintained at 30° C on either enriched yeast extract (1%)-peptone (2%) based medium supplemented with 2% glucose (YPD), or synthetic complete medium (SC) supplemented with 2% glucose and the appropriate amino acids to maintain selection (7). Cells cultured on solid media plates were done so with YPD or SC media supplemented with 2% agar (7). Selection for yeast strains containing the KanMX4 marker was done with YPD agar plates supplemented with G418 (200 µg/mL) (7). WT cells treated with the heme synthesis inhibitor, succinylacetone (SA), and *hem1Δ* cells were cultured in YPD or SC media supplemented with 50 µg/mL of 5-aminolevulinic acid (ALA) or 15 mg/mL of ergosterol and 0.5% Tween-80 (YPDE or SCE, respectively) (79) (7).

#### ***Labile heme and total heme depletion***

In order to sequester labile heme in the cytosol, we generated a WT yeast strain expressing an episomal plasmid (p316-GAL) containing an allele of the high affinity hemoprotein Cytochrome *b*<sub>562</sub> (Cyt *b*<sub>562</sub>) driven by the galactose-inducible promoter (pGAL); the plasmid is referred to as pGAL-Cyt *b*<sub>562</sub>. A control strain expressing the empty vector (EV), (pGAL-EV), was also generated. For labile heme measurements, the strains expressing pGAL-Cyt *b*<sub>562</sub> or pGAL-EV also co-expressed the previously described heme sensor, HS1-M7A, using an episomal plasmid (pRS415) that drives sensor expression with the *GPD* promoter (7). For Hap1 activity measurements, the strains expressing pGAL-Cyt *b*<sub>562</sub> or pGAL-EV also co-expressed the previously described p*CYC1-eGFP* Hap1 reporter, which is an episomal plasmid (pRS415) that drives *eGFP* expression using the *CYC1* promoter, a transcriptional target of Hap1 (7). In order to induce Cyt *b*<sub>562</sub> expression, cells were cultured in SC-URA-LEU media to maintain selection of both Cyt *b*<sub>562</sub> and the heme sensor, HS1-M7A, or p*CYC1-eGFP*. Instead of using 2% glucose, which will repress the expression of the GAL-inducible promoter, we cultured cells in 2% raffinose and either 0.1% galactose (inducing conditions) or vehicle (sterile water, non-inducing conditions). Parallel control cultures were treated with 500 µM succinylacetone (SA) in order to deplete intracellular heme. All cultures were seeded at an

initial optical density of OD<sub>600nm</sub> = .005 and cultured until cells reached a final density of OD<sub>600nm</sub> ~ 1.0, which typically took 14-16 hours. Following growth, cells were harvested, washed, and resuspended in phosphate-buffered saline (PBS) and sensor or eGFP fluorescence was measured as described in “***Labile heme quantification***” and “***Hap1 activity***”.

In order to deplete total heme, cells were cultured with the indicated concentrations of the heme biosynthetic inhibitor, succinylacetone (SA), in an appropriate SCE drop-out media. All cultures were seeded at an initial optical density of OD<sub>600nm</sub> = .005 and cultured until cells reached a final density of OD<sub>600nm</sub> ~ 1.0, which typically took 14-16 hours. Following growth, cells were harvested, washed, and processed for determination of labile or total heme as described in “***Labile heme quantification***” and “***Total heme quantification***”.

#### ***Yeast model of Pb<sup>2+</sup> toxicity***

Due to the insolubility of Pb(NO<sub>3</sub>)<sub>2</sub> in yeast media, we subjected exponential phase yeast cells to varying doses of Pb<sup>2+</sup> in MES buffer for 3 hours, a media in which Pb(NO<sub>3</sub>)<sub>2</sub> is soluble. Cells were pre-cultured in an appropriate SC drop-out media to a final density of OD<sub>600nm</sub> ~ 1.0. Following washing with sterile water, cells were resuspended in 10 mM MES buffer containing varying concentrations of Pb(NO<sub>3</sub>)<sub>2</sub> at a density of 1 OD/mL, and mixed every 15 minutes at 25° C for 3 hours. Following exposure to Pb<sup>2+</sup> in MES buffer, cells were thoroughly washed with sterile water, resuspended in an appropriate SC drop-out mixture to a final density of OD<sub>600nm</sub> ~ 1.0 and allowed to recover for 4 hours, while shaking at 220 RPM at 30° C. Cell viability was measured by diluting the cells to an initial density of OD<sub>600nm</sub> = 0.01 in an appropriate SC drop-out media after the recovery phase and solution turbidity was recorded by measuring OD<sub>600nm</sub> after 20 hours of growth shaking at 220 RPM and 30° C.

In order to assess the effects of Pb<sup>2+</sup> toxicity in an anaerobic environment, the Pb<sup>2+</sup> toxicity model described above was modified as follows: the Pb<sup>2+</sup> exposure in MES buffer was accomplished in de-gassed MES buffer with varying concentrations of Pb<sup>2+</sup> in a COY anaerobic chamber maintained with an inert atmosphere of 95% N<sub>2</sub> and 5% H<sub>2</sub>. Following Pb<sup>2+</sup> exposure, cells were washed with sterile de-gassed water and

allowed to recover in de-gassed SC media, all anaerobically in the COY anaerobic chamber. Cell viability was measured by diluting the anaerobic cultures into an appropriate SC drop-out media after the recovery phase and solution turbidity was recorded by measuring OD<sub>600nm</sub> after 16 hours of growth shaking at 220 RPM and 30° C in air.

All analytical analyses, including for labile or total heme, was conducted immediately after the 3 hour Pb<sup>2+</sup> exposure in MES buffer (pre-recovery) or after the 4 hour recovery in SC media (post-recovery).

### Viability measurements using FUN-1

Cells were grown as indicated in “**Yeast model of Pb<sup>2+</sup> toxicity**”. After conditioning cells in MES buffer with or without Pb<sup>2+</sup>, 1 O.D. of cells were pelleted, washed once with 1 mL sterile MilliQ water, and once with 500 µL of 10 mM HEPES with 2% Glucose (w/v) (HG Buffer). Cells were pelleted again then resuspended in 300 µL of HG buffer, then treated with 24.5 µL of 200 µM FUN-1 (Thermo-Fisher) to a final concentration of 15 µM. The 200 µM FUN-1 working stock solution was prepared by diluting a 10 mM DMSO FUN-1 stock solution into HG buffer. Cells were allowed to incubate in the dark at 30° C for 30 minutes and then washed three times in HG buffer. Cells were imaged on glass slides with cover slips using the Cytation 3 imaging plate reader (Biotek) with eGFP and TexasRed Filter Cubes. In stained cells, the observation of red puncta was used to score viable cells and the observation of diffuse green fluorescence was used to score dead cells. On average, ~100 cells were analyzed per sample.

### Labile heme quantification

Measurements of labile heme were accomplished as previously described (7). For all heme sensor fluorescence measurements, following cell growth, cells were washed in water and resuspended in phosphate-buffered saline (PBS) at a density between 3 and 5 OD<sub>600nm</sub>/mL, or 6 x 10<sup>7</sup> to 1 x 10<sup>8</sup> cells/mL. Fluorescence was recorded on a Synergy Mx multi-modal plate reader using black Greiner Bio-one flat bottom fluorescence plates. eGFP and mKATE2 fluorescence was recorded using excitation and emission wavelength pairs of 488 nm and 510 nm and 588 nm and 620 nm, respectively. Background fluorescence of cells not expressing the heme

sensors were recorded and subtracted from the eGFP and mKATE2 fluorescence values. The sensor eGFP/mKATE2 fluorescence ratio ( $R_{\text{expt}}$ ) is a qualitative indicator of labile or bioavailable heme, with a low ratio indicating a high concentration of labile heme and a high ratio indicating a low concentration of labile heme.

For quantitative labile heme monitoring, we can convert  $R_{\text{expt}}$  values to the fractional heme saturation of the sensor (% Heme Bound) (**Equation 1**) or, if the sensor heme dissociation constant is known ( $K_D$ ), the concentration of labile heme (**Equation 2**). Both metrics require that the eGFP/mKATE2 sensor fluorescence ratio is known when the sensor is 100% bound ( $R_{\text{max}}$ ) or 0% bound ( $R_{\text{min}}$ ) (7). Based on a 1:1 heme-binding model, the fractional saturation, % Bound, of the sensor can be calculated according to **Equation 1** (7):

$$[\% \text{ Bound}] = ([R - R_{\text{min}}] / [R_{\text{max}} - R_{\text{min}}]) * 100$$

### Equation 1

The labile heme concentration can be calculated according to **Equation 2** (7,80):

$$[\text{heme}] = \frac{K_D \times ([R_{\text{expt}} - R_{\text{min}}] / [R_{\text{max}} - R_{\text{expt}}]) \times (F_{\text{mKATE2}}^{\text{min}} / F_{\text{mKATE2}}^{\text{max}})}{\text{Equation 2}}$$

$R_{\text{expt}}$  is the eGFP/mKATE2 fluorescence ratio under any given experimental condition,  $R_{\text{min}}$  is the eGFP/mKATE2 fluorescence ratio when 0% of the sensor is bound to heme,  $R_{\text{max}}$  is the eGFP/mKATE2 fluorescence ratio when 100% of the sensor is bound to heme,  $F_{\text{mKATE2}}^{\text{min}}$  is the mKATE2 emission intensity when 0% of the sensor is bound to heme, and  $F_{\text{mKATE2}}^{\text{max}}$  is the mKATE2 emission intensity when 100% of the sensor is bound to heme. The  $F_{\text{mKATE2}}^{\text{min}} / F_{\text{mKATE2}}^{\text{max}}$  ratio is typically taken to be 1 given that mKATE2 fluorescence emission is not significantly perturbed upon heme binding to the sensor (7). Determination of  $R_{\text{max}}$  and  $F_{\text{mKATE2}}^{\text{max}}$  involves recording eGFP and mKATE2 fluorescence after digitonin permeabilization of cells and incubation with 50 µM heme. Briefly, 3 to 5 OD<sub>600nm</sub>/mL of cells are resuspended in PBS with 100 µg/mL of digitonin, 1 mM ascorbate, and 50 µM hemin chloride. After a 30 minute

incubation at 30°C, cells are harvested, washed, and resuspended in PBS buffer prior to recording of fluorescence. Given that the high affinity heme sensor, HS1, is quantitatively saturated with heme and its fluorescence properties are virtually identical to HS1-M7A, we can also determine  $R_{\max}$  and  $F^{\text{mKATE2}}_{\max}$  from parallel WT cultures expressing HS1 (7). Determination of  $R_{\min}$  and  $F^{\text{mKATE2}}_{\min}$  involves recording eGFP and mKATE2 fluorescence after cells are treated with the heme biosynthesis inhibitor succinylacetone (SA) (21) or from *hem1Δ* cells cultured in parallel (7).

### Total heme quantification

Measurements of total heme were accomplished using a fluorimetric assay designed to measure the fluorescence of protoporphyrin IX upon the release of iron from heme as previously described (81). For all total heme measurements, following cell growth,  $2 \times 10^8$  cells were harvested, washed in sterile water, and resuspended in 500  $\mu\text{L}$  of 20 mM oxalic acid and stored in a closed box at 4 °C overnight (16-18 hours). Next, an equal volume (500  $\mu\text{L}$ ) of 2 M oxalic acid was added to the cell suspensions in 20 mM oxalic acid. The samples were split, with half the cell suspension transferred to a heat block set at 95 °C and heated for 30 minutes and the other half of the cell suspension kept at room temperature (~25 °C) for 30 minutes. All suspensions were centrifuged for 2 minutes on a table-top microfuge at 21000  $\times$  g and the porphyrin fluorescence (ex: 400 nm, em: 620 nm) of 200  $\mu\text{L}$  of each sample was recorded on a Synergy Mx multi-modal plate reader using black Greiner Bio-one flat bottom fluorescence plates. Heme concentrations were calculated from a standard curve prepared by diluting 500-1500  $\mu\text{M}$  hemin chloride stock solutions in 0.1 M NaOH into MilliQ water, which was then added back to extra cell samples as prepared above. In order to calculate heme concentrations, the fluorescence of the unboiled sample (taken to be the background level of protoporphyrin IX) is subtracted from the fluorescence of the boiled sample (taken to be the free base porphyrin generated upon the release of heme iron). The cellular concentration of heme is determined by dividing the moles of heme determined in this fluorescence assay and dividing by the number of cells analyzed, giving moles of heme per cell, and then converting to a cellular concentration by dividing by the volume of a yeast

cell, taken to be 50 fL (7). This fluorescence assay gives similar qualitative trends between samples as an HPLC assay for heme we previously employed (7), but the absolute concentrations tend to be consistently 3-5 fold higher (data not shown).

### Hap1 activity

After growth, cells expressing p415-*CYC1-eGFP*, or *eGFP* driven by the Hap1 regulated *CYC1* promoter, were washed in sterile water and resuspended in PBS to a concentration of  $1 \times 10^8$  cells/mL and 100  $\mu\text{L}$  was used to measure eGFP fluorescence (ex. 488 nm, em. 510 nm). Background auto-fluorescence of cells not expressing eGFP was recorded and subtracted from the p415-*CYC1-eGFP* expressing strains. In order to account for heme/Hap1 independent changes in eGFP expression/fluorescence, we also cultured cells expressing p415-*GPD-eGFP*, a plasmid expressing eGFP under control of the heme/Hap1 independent *GPD* promoter.

### Immunoblotting

After culturing, cells were harvested, washed in ice-cold MilliQ water, and lysed in two pellet volumes of phosphate buffer supplemented with protease inhibitors as described previously (7,82). Lysis was achieved at 4 °C using one pellet volume of zirconium oxide beads and a bead beater (Bullet Blender, Next Advance) on a setting of 8 for 3 minutes (7). Lysate protein concentrations were determined by the Bradford method (Bio-rad) and 14% tris-glycine gels (Invitrogen) were employed for SDS-PAGE (7).  $\alpha$ -GAPDH rabbit polyclonal antibodies (Genetex, GTX100118) and a goat  $\alpha$ -rabbit secondary antibody conjugated to a 680 nm emitting fluorophore (Biotium) were used to probe for GAPDH. Yeast cytosolic catalase, Ctt1p, was probed using a custom antibody generated by Genscript's custom antibody service (Poly Express Premium Service, SC1676). An  $\alpha$ -Ctt1p antibody was raised in rabbit against a 1-320 amino acid fragment of Ctt1p. The  $\alpha$ -Ctt1p antibody was validated in yeast by comparing immunoreactivity between WT, *ctt1Δ*, and *cta1Δ* cells, the latter being a deletion mutant of a peroxisomal/mitochondrial catalase, Cta1p, unrelated to Ctt1p (**Fig. S5**). All gels were imaged on a LiCOR Odyssey Infrared imager (7,82).

### **Catalase activity**

After culturing, cells were harvested and lysed in phosphate buffer and 10  $\mu$ g of protein lysate were subjected to native PAGE on a 10% tris-glycine gel (Invitrogen). After electrophoresis, an in-gel activity stain was utilized to measure catalase activity (7,83). Briefly, a catalase staining solution containing 1 part Dopamine (20mg/mL) in pH 8 0.2 M KPi buffer, 1 part para-phenylenediamine (3.5mg/mL) in pH 8 0.2M KPi, 1 part 15% H<sub>2</sub>O<sub>2</sub>, and 2 parts DMSO were mixed in the order listed. The staining solution was added directly to the gel and allowed to stain for 2 minutes, followed by rinsing in MilliQ water and imaging.

### **Plasmids**

All yeast expression plasmids used in this study are listed in **Table S1** and were previously described, except for pDH039, the plasmid expressing Cytochrome *b*<sub>562</sub> (Cyt *b*<sub>562</sub>) driven by a galactose (GAL)-inducible promoter, pGAL-Cyt *b*<sub>562</sub>. This plasmid was constructed by amplifying the coding sequence of Cyt *b*<sub>562</sub> from the HSI sensor (7). The following primers were utilized to amplify a BamHI/XbaI fragment of Cyt *b*<sub>562</sub>:

prDH025: 5'-  
CCTTTGGTGGCTCTGGATCCATGGCAGATC  
TGGAAGACAACATGG-3'

prDH026:  
5'GGTCAGTTTGCCACCTCTAGATCATCTGT  
ATTCTGATGATATGC-3'

Following amplification and digestion with BamHI and XbaI, the Cyt *b*<sub>562</sub> coding sequence was ligated into BamHI and XbaI digested p316-GAL1 (17). The amino acid sequence of Cyt *b*<sub>562</sub> is as follows, with the heme coordinating residues highlighted in red:

ADLEDNMETLNDNLKVIEKADNAAQ  
VKDALTKMRAAALDAQATPPKLEDKSPDS  
PEMKDFRHGFDILVGQIDDALKLANEGKVK  
EAQAAAEQLKTRNAYHQYR

### **Total reflection X-ray fluorescence (TXRF) spectroscopy**

Elemental analysis of cells, and in particular metal analysis of Pb, 1<sup>st</sup> row transition elements, P, and S, were accomplished by total reflection x-ray fluorescence (TXRF) on a Bruker

S2 Picofox TXRF as described previously (7). Briefly, following growth, cells were washed sequentially in ice-cold Tris-EDTA (TE), pH 8.0 buffer and MiliQ water, and then finally resuspended in MiliQ water to a density of  $2 \times 10^9$  cells/mL. 2  $\mu$ L of a cell suspension, spiked with 1 ppm of a Ga internal standard, were spotted onto a quartz sample disc, and atomic fluorescence emission spectra were collected according to the manufacturer's recommendations (7). The cellular metal concentrations were determined by assuming a yeast cell volume of 50 fL and that a solution turbidity of OD<sub>600nm</sub> = 1.0 is equivalent to  $2 \times 10^7$  cells/mL (7).

### **In-gel protein digestion**

In-gel protein digestion was conducted as previously described (84), with modifications. Briefly, selected protein bands were excised from the Coomassie-stained gel, diced into small pieces, and then de-stained with HPLC-grade water (Avantor) and 1:1 acetonitrile (ACN)/ammonium bicarbonate (ABC) (Sigma-Aldrich). The de-stained gel pieces were then dehydrated with multiple ACN washes until rock hard, followed by air drying for ~15 minutes. The gel pieces were rehydrated for 30 minutes with 10 mM dithiothreitol (Sigma-Aldrich) to reduce disulfide bonds, followed by replacement with 55mM iodoacetic acid (Sigma-Aldrich) and 45 minutes shaking at 750 rpm in the dark to alkylate the reduced thiols. After reduction/alkylation, the gel pieces were once again washed and dehydrated as before, and then chilled on ice for 15 minutes. To the chilled gel pieces, 30 $\mu$ L of 20 $\mu$ g/mL sequencing grade modified trypsin (Promega) was added for 30 minutes on ice. Excess trypsin solution was then removed and replaced with 100  $\mu$ L 50mM ABC and the pieces were incubated overnight at 37°C with shaking at 750 rpm. Resultant proteolytic peptides were extracted by two rounds of dehydration using 100 $\mu$ L ACN and collection of the resulting extract into low-retention microfuge tubes, which were frozen solid at -80°C and then sublimated by centri-vapping. The dried peptides were reconstituted by sonication in 5% ACN/0.1% formic acid and stored at -80°C prior to analysis.

### **Mass spectrometry**



LC-MS analysis of peptides produced by in-gel digestion was carried out with an UltiMate™ 3000 RSLCnano System UPLC system (Dionex) with Acclaim PepMap RSLC column (75mm x 25cm nanoViper C18 2mm, 100Å) coupled to a Q-Exactive Plus Orbitrap mass spectrometer (Thermo Scientific) run in data-dependent acquisition mode (top-15). Resultant RAW files were analyzed using Proteome Discoverer 2.1 with embedded SEQUEST search algorithm operating with an allowable 1% false-discovery rate, wherein the *Saccharomyces cerevisiae* protein sequence database was used as the target for spectral matching. Only high confidence peptide spectral matches were used for protein identification and are reported below (**Table S2**).

## **Acknowledgements**

This work was supported by the U.S. National Institutes of Health (ES025661 to A.R.R. and GM118744 to A.R.R. with sub-award to M.P.T.), the U.S. National Science Foundation (MCB-1552791 to A.R.R.), the Blanchard Professorship (to A.R.R.) and start-up funding from the Georgia Institute of Technology (to A.R.R. and to M.P.T.). R. H. was supported by the Petit Institute Scholarship. We thank Dr. Rebecca Donegan for assistance in developing the porphyrin fluorescence assay for total heme.

**Conflict of interest:** The authors declare that they have no conflicts of interest with the contents of this article.

**Author contributions:** DAH, RH, HK, OMG, MPT, and ARR designed research. DAH, RH, HK, OMG and ARR performed research. All authors analyzed data. DAH and ARR wrote the paper with input from all co-authors.

## References

1. Reddi, A. R., and Hamza, I. (2016) Heme Mobilization in Animals: A Metallolipid's Journey. *Acc Chem Res* **49**, 1104-1110
2. Hanna, D. A., Martinez-Guzman, O., and Reddi, A. R. (2017) Heme Gazing: Illuminating Eukaryotic Heme Trafficking, Dynamics, and Signaling with Fluorescent Heme Sensors. *Biochemistry* **56**, 1815-1823
3. Severance, S., and Hamza, I. (2009) Trafficking of heme and porphyrins in metazoa. *Chem Rev* **109**, 4596-4616
4. Hamza, I., and Dailey, H. A. (2012) One ring to rule them all: trafficking of heme and heme synthesis intermediates in the metazoans. *Biochim Biophys Acta* **1823**, 1617-1632
5. Sassa, S. (2004) Why heme needs to be degraded to iron, biliverdin IXalpha, and carbon monoxide? *Antioxid Redox Signal* **6**, 819-824
6. Kumar, S., and Bandyopadhyay, U. (2005) Free heme toxicity and its detoxification systems in human. *Toxicol Lett* **157**, 175-188
7. Hanna, D. A., Harvey, R. M., Martinez-Guzman, O., Yuan, X., Chandrasekharan, B., Raju, G., Outten, F. W., Hamza, I., and Reddi, A. R. (2016) Heme dynamics and trafficking factors revealed by genetically encoded fluorescent heme sensors. *Proc Natl Acad Sci U S A* **113**, 7539-7544
8. Pfeifer, K., Kim, K. S., Kogan, S., and Guarente, L. (1989) Functional dissection and sequence of yeast HAP1 activator. *Cell* **56**, 291-301
9. Zhang, L., Bermingham-McDonogh, O., Turcotte, B., and Guarente, L. (1993) Antibody-promoted dimerization bypasses the regulation of DNA binding by the heme domain of the yeast transcriptional activator HAP1. *Proc Natl Acad Sci U S A* **90**, 2851-2855
10. Zhang, L., and Hach, A. (1999) Molecular mechanism of heme signaling in yeast: the transcriptional activator Hap1 serves as the key mediator. *Cell Mol Life Sci* **56**, 415-426
11. Zhang, L., Hach, A., and Wang, C. (1998) Molecular mechanism governing heme signaling in yeast: a higher-order complex mediates heme regulation of the transcriptional activator HAP1. *Mol Cell Biol* **18**, 3819-3828
12. Feng, Y., Sligar, S. G., and Wand, A. J. (1994) Solution structure of apocytochrome b562. *Nat Struct Biol* **1**, 30-35
13. Feng, Y. Q., and Sligar, S. G. (1991) Effect of heme binding on the structure and stability of Escherichia coli apocytochrome b562. *Biochemistry* **30**, 10150-10155
14. Itagaki, E., Palmer, G., and Hager, L. P. (1967) Studies on cytochrome b562 of Escherichia coli. II. Reconstitution of cytochrome b562 from apoprotein and hemin. *J Biol Chem* **242**, 2272-2277
15. Nikkila, H., Gennis, R. B., and Sligar, S. G. (1991) Cloning and expression of the gene encoding the soluble cytochrome b562 of Escherichia coli. *Eur J Biochem* **202**, 309-313
16. Robinson, C. R., Liu, Y., Thomson, J. A., Sturtevant, J. M., and Sligar, S. G. (1997) Energetics of heme binding to native and denatured states of cytochrome b562. *Biochemistry* **36**, 16141-16146
17. Kiktev, D. A., Patterson, J. C., Muller, S., Bariar, B., Pan, T., and Chernoff, Y. O. (2012) Regulation of chaperone effects on a yeast prion by cochaperone Sgt2. *Mol Cell Biol* **32**, 4960-4970
18. Barker, P. D., Nerou, E. P., Cheesman, M. R., Thomson, A. J., de Oliveira, P., and Hill, H. A. (1996) Bis-methionine ligation to heme iron in mutants of cytochrome b562. 1. Spectroscopic and electrochemical characterization of the electronic properties. *Biochemistry* **35**, 13618-13626
19. Reddi, A. R., Reedy, C. J., Mui, S., and Gibney, B. R. (2007) Thermodynamic investigation into the mechanisms of proton-coupled electron transfer events in heme protein maquettes. *Biochemistry* **46**, 291-305
20. Conant, J. B., and Tongberg, C. O. (1930) The oxidation-reduction potentials of hemin and related substances: I. The potentials of various hemins and hematins in the absence and presence of pyridine. *Journal of Biological Chemistry* **86**, 733-741

21. Ebert, P. S., Hess, R. A., Frykholm, B. C., and Tschudy, D. P. (1979) Succinylacetone, a potent inhibitor of heme biosynthesis: effect on cell growth, heme content and delta-aminolevulinic acid dehydratase activity of malignant murine erythroleukemia cells. *Biochem Biophys Res Commun* **88**, 1382-1390
22. Sassa, S., and Kappas, A. (1982) Succinylacetone inhibits delta-aminolevulinate dehydratase and potentiates the drug and steroid induction of delta-aminolevulinate synthase in liver. *Trans Assoc Am Physicians* **95**, 42-52
23. Correia, M. A., Sinclair, P. R., and De Matteis, F. (2011) Cytochrome P450 regulation: the interplay between its heme and apoprotein moieties in synthesis, assembly, repair, and disposal. *Drug Metab Rev* **43**, 1-26
24. De Matteis, F., Gibbs, A. H., and Smith, A. G. (1980) Inhibition of protohaem ferro-lyase by N-substituted porphyrins. Structural requirements for the inhibitory effect. *Biochem J* **189**, 645-648
25. De Matteis, F., and Marks, G. S. (1983) The effect of N-methylprotoporphyrin and succinylacetone on the regulation of heme biosynthesis in chicken hepatocytes in culture. *FEBS Lett* **159**, 127-131
26. Ortiz de Montellano, P. R., Mico, B. A., and Yost, G. S. (1978) Suicidal inactivation of cytochrome P-450. Formation of a heme-substrate covalent adduct. *Biochem Biophys Res Commun* **83**, 132-137
27. Smith, A. G., Clothier, B., Carthew, P., Childs, N. L., Sinclair, P. R., Nebert, D. W., and Dalton, T. P. (2001) Protection of the Cyp1a2(-/-) null mouse against uroporphyrin and hepatic injury following exposure to 2,3,7,8-tetrachlorodibenzo-p-dioxin. *Toxicol Appl Pharmacol* **173**, 89-98
28. Urquhart, A. J., Elder, G. H., Roberts, A. G., Lambrecht, R. W., Sinclair, P. R., Bement, W. J., Gorman, N., and Sinclair, J. A. (1988) Uroporphyrin produced in mice by 20-methylcholanthrene and 5-aminolaevulinic acid. *Biochem J* **253**, 357-362
29. Schauder, A., Avital, A., and Malik, Z. (2010) Regulation and gene expression of heme synthesis under heavy metal exposure--review. *J Environ Pathol Toxicol Oncol* **29**, 137-158
30. Sharma, B., Singh, S., and Siddiqi, N. J. (2014) Biomedical implications of heavy metals induced imbalances in redox systems. *Biomed Res Int* **2014**, 640754
31. Lubran, M. M. (1980) Lead toxicity and heme biosynthesis. *Ann Clin Lab Sci* **10**, 402-413
32. Cohen, A. R., Trotzky, M. S., and Pincus, D. (1981) Reassessment of the microcytic anemia of lead poisoning. *Pediatrics* **67**, 904-906
33. Wani, A. L., Ara, A., and Usmani, J. A. (2015) Lead toxicity: a review. *Interdiscip Toxicol* **8**, 55-64
34. Flora, G., Gupta, D., and Tiwari, A. (2012) Toxicity of lead: A review with recent updates. *Interdiscip Toxicol* **5**, 47-58
35. Alam, J., Cai, J., and Smith, A. (1994) Isolation and characterization of the mouse heme oxygenase-1 gene. Distal 5' sequences are required for induction by heme or heavy metals. *J Biol Chem* **269**, 1001-1009
36. Gozzelino, R., Jeney, V., and Soares, M. P. (2010) Mechanisms of cell protection by heme oxygenase-1. *Annu Rev Pharmacol Toxicol* **50**, 323-354
37. Van der Heggen, M., Martins, S., Flores, G., and Soares, E. V. (2010) Lead toxicity in *Saccharomyces cerevisiae*. *Appl Microbiol Biotechnol* **88**, 1355-1361
38. Qian, Z. M., and Morgan, E. H. (1990) Effect of lead on the transport of transferrin-free and transferrin-bound iron into rabbit reticulocytes. *Biochem Pharmacol* **40**, 1049-1054
39. Fu, X., Zeng, A., Zheng, W., and Du, Y. (2014) Upregulation of zinc transporter 2 in the blood-CSF barrier following lead exposure. *Exp Biol Med (Maywood)* **239**, 202-212
40. Pounds, J. G. (1984) Effect of lead intoxication on calcium homeostasis and calcium-mediated cell function: a review. *Neurotoxicology* **5**, 295-331
41. Quintanar-Escorza, M. A., Gonzalez-Martinez, M. T., del Pilar, I. O., and Calderon-Salinas, J. V. (2010) Oxidative damage increases intracellular free calcium [Ca<sup>2+</sup>]<sub>i</sub> concentration in human erythrocytes incubated with lead. *Toxicol In Vitro* **24**, 1338-1346



42. Zheng, G., Zhang, J., Xu, Y., Shen, X., Song, H., Jing, J., Luo, W., Zheng, W., and Chen, J. (2014) Involvement of CTR1 and ATP7A in lead (Pb)-induced copper (Cu) accumulation in choroidal epithelial cells. *Toxicol Lett* **225**, 110-118
43. Dongre, N. N., Suryakar, A. N., Patil, A. J., Hundekari, I. A., and Devarnavadagi, B. B. (2013) Biochemical effects of lead exposure on battery manufacture workers with reference to blood pressure, calcium metabolism and bone mineral density. *Indian J Clin Biochem* **28**, 65-70
44. Schulze, H., and Brand, J. J. (1978) Lead toxicity and phosphate deficiency in chlamydomonas. *Plant Physiol* **62**, 727-730
45. Jaishankar, M., Tseten, T., Anbalagan, N., Mathew, B. B., and Beeregowda, K. N. (2014) Toxicity, mechanism and health effects of some heavy metals. *Interdiscip Toxicol* **7**, 60-72
46. Mendoza-Cozatl, D., Loza-Tavera, H., Hernandez-Navarro, A., and Moreno-Sanchez, R. (2005) Sulfur assimilation and glutathione metabolism under cadmium stress in yeast, protists and plants. *FEMS Microbiol Rev* **29**, 653-671
47. Ernst, W. H., Krauss, G. J., Verkleij, J. A., and Wesenberg, D. (2008) Interaction of heavy metals with the sulphur metabolism in angiosperms from an ecological point of view. *Plant Cell Environ* **31**, 123-143
48. Protchenko, O., and Philpott, C. C. (2003) Regulation of intracellular heme levels by HMX1, a homologue of heme oxygenase, in *Saccharomyces cerevisiae*. *J Biol Chem* **278**, 36582-36587
49. Collinson, E. J., Wimmer-Kleikamp, S., Gerega, S. K., Yang, Y. H., Parish, C. R., Dawes, I. W., and Stocker, R. (2011) The yeast homolog of heme oxygenase-1 affords cellular antioxidant protection via the transcriptional regulation of known antioxidant genes. *J Biol Chem* **286**, 2205-2214
50. Protchenko, O., Shakoury-Elizeh, M., Keane, P., Storey, J., Androphy, R., and Philpott, C. C. (2008) Role of PUG1 in inducible porphyrin and heme transport in *Saccharomyces cerevisiae*. *Eukaryot Cell* **7**, 859-871
51. Elsasser, S., Chandler-Militello, D., Muller, B., Hanna, J., and Finley, D. (2004) Rad23 and Rpn10 serve as alternative ubiquitin receptors for the proteasome. *J Biol Chem* **279**, 26817-26822
52. Marques, M., Mojzita, D., Amorim, M. A., Almeida, T., Hohmann, S., Moradas-Ferreira, P., and Costa, V. (2006) The Pep4p vacuolar proteinase contributes to the turnover of oxidized proteins but PEP4 overexpression is not sufficient to increase chronological lifespan in *Saccharomyces cerevisiae*. *Microbiology* **152**, 3595-3605
53. Papinski, D., and Kraft, C. (2016) Regulation of Autophagy By Signaling Through the Atg1/ULK1 Complex. *J Mol Biol* **428**, 1725-1741
54. Liu, S. C., Zhai, S., and Palek, J. (1988) Detection of heme release during hemoglobin S denaturation. *Blood* **71**, 1755-1758
55. Aich, A., Freundlich, M., and Vekilov, P. G. (2015) The free heme concentration in healthy human erythrocytes. *Blood Cells Mol Dis* **55**, 402-409
56. Song, Y., Yang, M., Wegner, S. V., Zhao, J., Zhu, R., Wu, Y., He, C., and Chen, P. R. (2015) A Genetically Encoded FRET Sensor for Intracellular Heme. *ACS Chem Biol* **10**, 1610-1615
57. Bonkovsky, H. L., Healey, J. F., Lourie, A. N., and Gerson, G. G. (1991) Intravenous heme-albumin in acute intermittent porphyria: evidence for repletion of hepatic hemoproteins and regulatory heme pools. *Am J Gastroenterol* **86**, 1050-1056
58. Zhang, T., Bu, P., Zeng, J., and Vancura, A. (2017) Increased heme synthesis in yeast induces a metabolic switch from fermentation to respiration even under conditions of glucose repression. *J Biol Chem* **292**, 16942-16954
59. Tu, B. P., Mohler, R. E., Liu, J. C., Dombek, K. M., Young, E. T., Synovec, R. E., and McKnight, S. L. (2007) Cyclic changes in metabolic state during the life of a yeast cell. *Proc Natl Acad Sci U S A* **104**, 16886-16891
60. Tu, B. P., and McKnight, S. L. (2009) Evidence of carbon monoxide-mediated phase advancement of the yeast metabolic cycle. *Proc Natl Acad Sci U S A* **106**, 14293-14296

61. Raghuram, S., Stayrook, K. R., Huang, P., Rogers, P. M., Nosie, A. K., McClure, D. B., Burris, L. L., Khorasanizadeh, S., Burris, T. P., and Rastinejad, F. (2007) Identification of heme as the ligand for the orphan nuclear receptors REV-ERB $\alpha$  and REV-ERB $\beta$ . *Nat Struct Mol Biol* **14**, 1207-1213
62. Sousa, C. A., and Soares, E. V. (2014) Mitochondria are the main source and one of the targets of Pb (lead)-induced oxidative stress in the yeast *Saccharomyces cerevisiae*. *Appl Microbiol Biotechnol* **98**, 5153-5160
63. Perez, R. R., Sousa, C. A., Vankeersbilck, T., Machado, M. D., and Soares, E. V. (2013) Evaluation of the role of glutathione in the lead-induced toxicity in *Saccharomyces cerevisiae*. *Curr Microbiol* **67**, 300-305
64. Lanphear, B. P., Burgoon, D. A., Rust, S. W., Eberly, S., and Galke, W. (1998) Environmental exposures to lead and urban children's blood lead levels. *Environ Res* **76**, 120-130
65. Piomelli, S., Seaman, C., Zullo, D., Curran, A., and Davidow, B. (1982) Threshold for lead damage to heme synthesis in urban children. *Proc Natl Acad Sci U S A* **79**, 3335-3339
66. Gillis, B. S., Arbieva, Z., and Gavin, I. M. (2012) Analysis of lead toxicity in human cells. *BMC Genomics* **13**, 344
67. Lidsky, T. I., and Schneider, J. S. (2003) Lead neurotoxicity in children: basic mechanisms and clinical correlates. *Brain* **126**, 5-19
68. Yedjou, C. G., Milner, J. N., Howard, C. B., and Tchounwou, P. B. (2010) Basic apoptotic mechanisms of lead toxicity in human leukemia (HL-60) cells. *Int J Environ Res Public Health* **7**, 2008-2017
69. Chen, C., and Wang, J. (2007) Response of *Saccharomyces cerevisiae* to lead ion stress. *Appl Microbiol Biotechnol* **74**, 683-687
70. Bussche, J. V., and Soares, E. V. (2011) Lead induces oxidative stress and phenotypic markers of apoptosis in *Saccharomyces cerevisiae*. *Appl Microbiol Biotechnol* **90**, 679-687
71. Wysocki, R., and Tamas, M. J. (2010) How *Saccharomyces cerevisiae* copes with toxic metals and metalloids. *FEMS Microbiol Rev* **34**, 925-951
72. Magyar, J. S., Weng, T. C., Stern, C. M., Dye, D. F., Rous, B. W., Payne, J. C., Bridgewater, B. M., Mijovilovich, A., Parkin, G., Zaleski, J. M., Penner-Hahn, J. E., and Godwin, H. A. (2005) Reexamination of lead(II) coordination preferences in sulfur-rich sites: implications for a critical mechanism of lead poisoning. *J Am Chem Soc* **127**, 9495-9505
73. Grunberg-Etkovitz, N., Lev, N., Ickowicz, D., Avital, A., Offen, D., and Malik, Z. (2009) Accelerated proteasomal activity induced by Pb<sup>2+</sup>, Ga<sup>3+</sup>, or Cu<sup>2+</sup> exposure does not induce degradation of alpha-synuclein. *J Environ Pathol Toxicol Oncol* **28**, 5-24
74. Guo, G. G., Gu, M., and Etlinger, J. D. (1994) 240-kDa proteasome inhibitor (CF-2) is identical to delta-aminolevulinic acid dehydratase. *J Biol Chem* **269**, 12399-12402
75. Vallelle, F., Deuel, J. W., Opitz, L., Schaer, C. A., Puglia, M., Lonn, M., Engelsberger, W., Schauer, S., Karnaukhova, E., Spahn, D. R., Stocker, R., Buehler, P. W., and Schaer, D. J. (2015) Proteasome inhibition and oxidative reactions disrupt cellular homeostasis during heme stress. *Cell Death Differ* **22**, 597-611
76. Lopes, A. C., Peixe, T. S., Mesas, A. E., and Paoliello, M. M. (2016) Lead Exposure and Oxidative Stress: A Systematic Review. *Rev Environ Contam Toxicol* **236**, 193-238
77. Lee, K. H., Lee, S. K., Kim, H. S., Cho, E. J., Joo, H. K., Lee, E. J., Lee, J. Y., Park, M. S., Chang, S. J., Cho, C. H., Park, J. B., and Jeon, B. H. (2009) Overexpression of Ref-1 Inhibits Lead-induced Endothelial Cell Death via the Upregulation of Catalase. *Korean J Physiol Pharmacol* **13**, 431-436
78. Gietz, R. D., and Schiestl, R. H. (1991) Applications of high efficiency lithium acetate transformation of intact yeast cells using single-stranded nucleic acids as carrier. *Yeast* **7**, 253-263
79. Ness, F., Achstetter, T., Duport, C., Karst, F., Spagnoli, R., and Degryse, E. (1998) Sterol uptake in *Saccharomyces cerevisiae* heme auxotrophic mutants is affected by ergosterol and oleate but not by palmitoleate or by sterol esterification. *J Bacteriol* **180**, 1913-1919

80. Grynkiewicz, G., Poenie, M., and Tsien, R. Y. (1985) A new generation of  $\text{Ca}^{2+}$  indicators with greatly improved fluorescence properties. *J Biol Chem* **260**, 3440-3450
81. Michener, J. K., Nielsen, J., and Smolke, C. D. (2012) Identification and treatment of heme depletion attributed to overexpression of a lineage of evolved P450 monooxygenases. *Proc Natl Acad Sci U S A* **109**, 19504-19509
82. Reddi, A. R., and Culotta, V. C. (2013) SOD1 integrates signals from oxygen and glucose to repress respiration. *Cell* **152**, 224-235
83. Baureder, M., and Hederstedt, L. (2012) Genes important for catalase activity in *Enterococcus faecalis*. *PLoS One* **7**, e36725
84. Shevchenko, A., Tomas, H., Havlis, J., Olsen, J. V., and Mann, M. (2006) In-gel digestion for mass spectrometric characterization of proteins and proteomes. *Nat Protoc* **1**, 2856-2860

## Figures

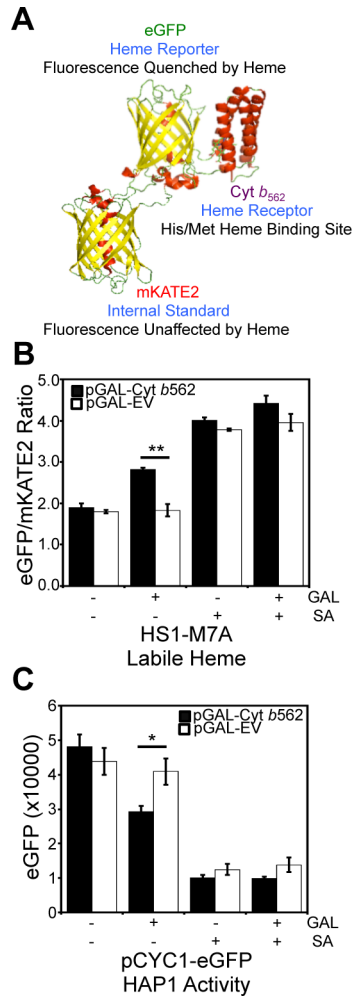


**Figure 1.** Over-expression of a high affinity hemoprotein, *Cyt b<sub>562</sub>*, attenuates labile heme and the activity of heme-regulated transcription factor, Hap1. (A) Molecular model and design principles of the heme sensor, HS1. Model derived from the X-ray structures of mKATE (PDB: 3BXX) and CG6 (PDB: 3U8P). (B) Cells expressing the heme sensor, HS1-M7A, and an allele of *Cyt b<sub>562</sub>* on a galactose (GAL)-inducible promoter (pGAL-*Cyt b<sub>562</sub>*) or empty vector (pGAL-EV) were cultured in 2% raffinose (RAF) with or without 1.0% galactose (GAL) or 500  $\mu$ M succinylacetone (SA) for 16 hours in SCE media. After growth, HS1-M7A sensor eGFP (ex. 488 nm, em. 510 nm) and mKATE2 (ex. 588 nm, em. 620 nm) fluorescence emission ratios were recorded. (C) Hap1 activity was measured in cells expressing pGAL-*Cyt b<sub>562</sub>* or pGAL-EV and cultured in 2% RAF with or without 1.0% GAL or 500  $\mu$ M SA for 16 hours in SC media using a transcriptional reporter consisting of an allele of *eGFP* driven by the *CYC1* promoter (pCYC1-*eGFP*), a Hap1 target gene. All data represent the mean  $\pm$  SD of triplicate cultures and the statistical significance was assessed using a two-sample t-test. \*  $P < 0.01$ , \*\*  $P < 0.001$ .



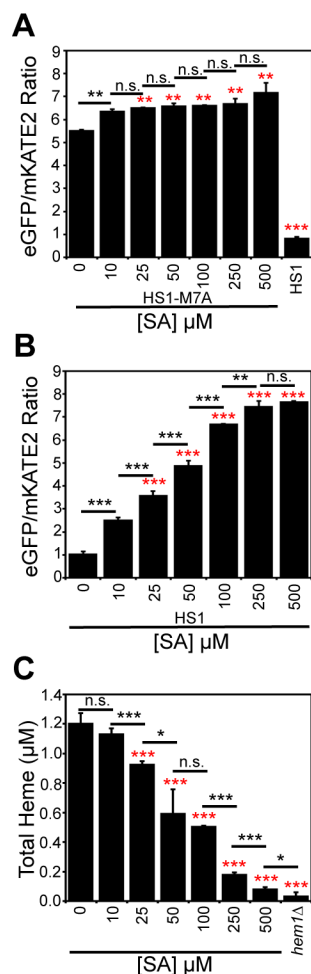


**Figure 2.** Labile heme (LH) is more sensitive to heme depletion using the heme biosynthetic inhibitor, succinylacetone (SA), than total heme. Labile heme was measured in HS1-M7A (A) or HS1 (B) expressing cells cultured in SCE media for 16 hours with the indicated concentration of SA prior to measurement of the eGFP/mKATE2 fluorescence ratios. (C) Total heme was measured in the cultures depicted in (A) or in heme deficient *hem1* $\Delta$  cells. All data represent the mean  $\pm$  SD of triplicate cultures and the statistical significance was assessed using a two-sample t-test. Black asterisks represent the statistical significance between the indicated pairwise comparisons of conditions and red asterisks represent the statistical significance relative to 0  $\mu$ M SA. \*  $P < 0.05$ , \*\*  $P < 0.005$ , \*\*\*  $P < 0.001$ , n.s. not significant.

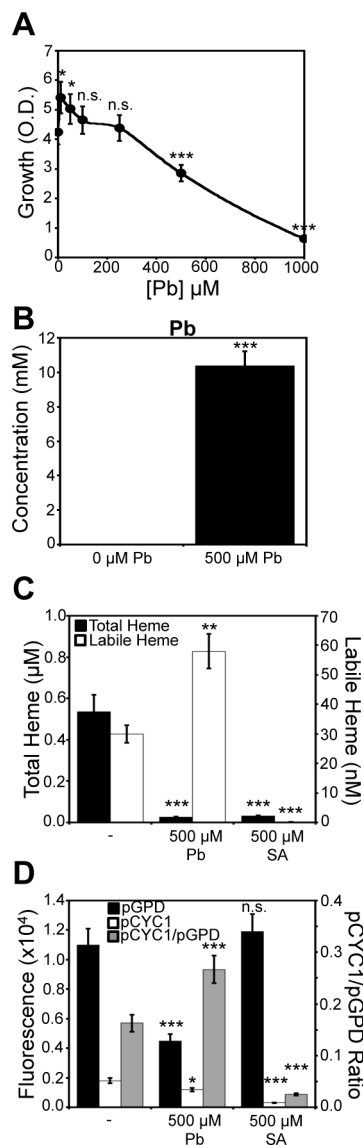


**Figure 3.** Labile heme and heme signaling is increased, but total heme is attenuated in response to  $\text{Pb}^{2+}$  toxicity. **(A)** Yeast cell viability, as measured by solution turbidity at an optical density (O.D.) of 600 nm, is diminished by exposure to  $\text{Pb}^{2+}$  in a dose-dependent manner. **(B)** At the  $\text{LD}_{50}$  dose of  $\text{Pb}^{2+}$  (500  $\mu\text{M}$ ), cells hyper-accumulate up to 10 mM  $\text{Pb}^{2+}$  as measured by total-reflection X-ray fluorescence (TXRF). **(C)** A dose of 500  $\mu\text{M}$   $\text{Pb}^{2+}$  diminishes total heme to levels similar to 500  $\mu\text{M}$  SA, but  $\text{Pb}^{2+}$  increases labile heme 2-fold whereas SA does not. **(D)** Hap1p activity in response to heme depletion by SA or  $\text{Pb}^{2+}$  is measured using the pCYC1-*eGFP* Hap1 reporter construct (pCYC1). In order to control for the effects of Hap1-independent effects of  $\text{Pb}^{2+}$  on *eGFP* expression, we measured *eGFP* fluorescence in response to  $\text{Pb}^{2+}$  or SA using an allele of *eGFP* driven by the heme/Hap1 independent promoter, *GPD* (pGPD). The ratio of pCYC1 to pGPD *eGFP* expression (pCYC1/pGPD) is a measure of heme/Hap1-specific activation of *CYC1*. All data represent the mean  $\pm$  SD of triplicate cultures and the statistical significance relative to untreated cells was assessed using a two-sample t-test. \*  $P < 0.05$ , \*\*  $P < 0.005$ , \*\*\*  $P < 0.001$ , n.s. not significant.

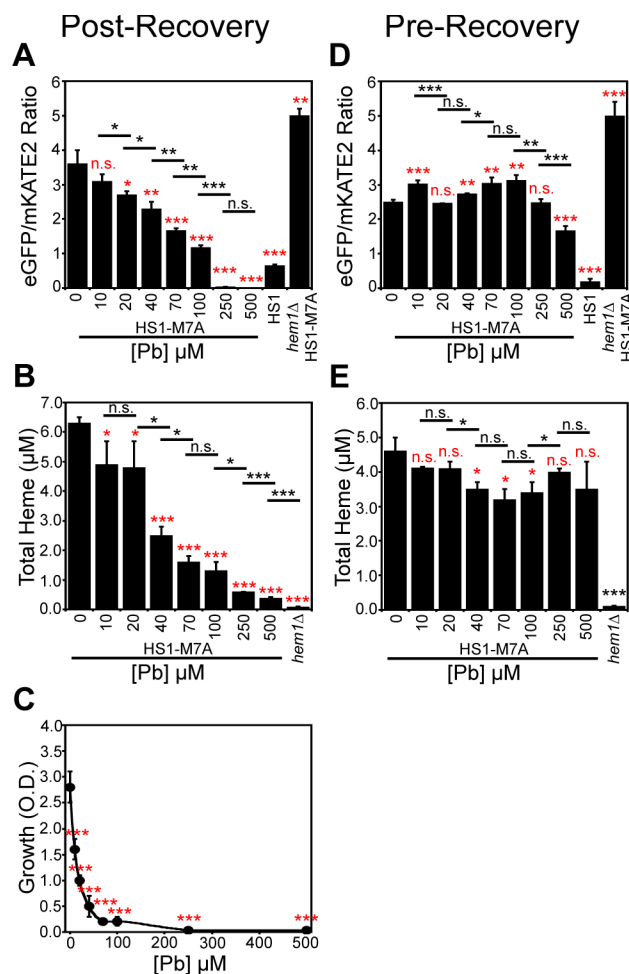


**Figure 4.**  $Pb^{2+}$  only perturbs total and labile heme after a recovery period following exposure to  $Pb^{2+}$ . In cells expressing HS1-M7A,  $Pb^{2+}$  (A) increases labile heme, (B) decreases total heme, (C) and diminishes cell viability in a dose-dependent manner if cells are allowed to recover for 4 hours in SCE media following  $Pb^{2+}$  exposure in MES buffer. However, (D) labile and (E) total heme in cells expressing HS1-M7A immediately after the exposure to  $Pb^{2+}$  in MES buffer is not significantly affected. All data represent the mean  $\pm$  SD of triplicate cultures and statistical significance was assessed using a two-sample t-test. Black asterisks represent the statistical significance between the indicated pairwise comparisons of conditions and red asterisks represent the statistical significance relative to 0  $\mu M$  [Pb]. \*  $P < 0.05$ , \*\*  $P < 0.005$ , \*\*\*  $P < 0.001$ , n.s. not significant.

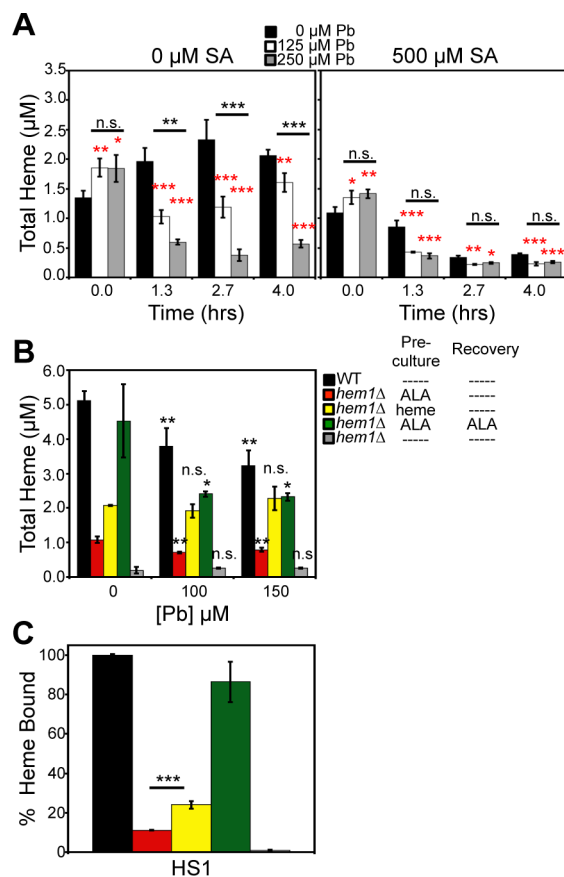


**Figure 5.**  $\text{Pb}^{2+}$ -dependent attenuation of total heme is largely dependent on heme synthesis. **(A)** WT cells untreated (left) or treated (right) with 500  $\mu\text{M}$  succinylacetone (SA) and the indicated concentrations of  $\text{Pb}^{2+}$  demonstrates that  $\text{Pb}^{2+}$  has a larger effect on depleting total heme in cells that can properly synthesize heme. **(B and C)** Endogenous heme, but not exogenous heme, is degraded in a  $\text{Pb}^{2+}$ -dependent manner. **(B)** Total and **(C)** labile heme was measured in HS1 expressing WT or *hem1* $\Delta$  cells conditioned with the indicated  $\text{Pb}^{2+}$  concentration and/or 200  $\mu\text{M}$  5-aminolevulinic acid (ALA) or 50  $\mu\text{M}$  hemin chloride during the pre-culture and/or post-  $\text{Pb}^{2+}$  recovery period. All data represent the mean  $\pm$  SD of triplicate cultures and statistical significance was assessed using a two-sample t-test. In panel **A**, black asterisks represent the statistical significance between the indicated pairwise comparisons of conditions and red asterisks represent the statistical significance relative to 0  $\mu\text{M}$  [Pb] for each time point. In panel **B**, black asterisks represent the statistical significance relative to 0  $\mu\text{M}$  [Pb] for each test condition. In panel **C**, the black asterisks represent the statistical significance between the indicated pairwise comparisons of strains. \*  $P < 0.05$ , \*\*  $P < 0.01$ , \*\*\*  $P < 0.001$ , n.s. not significant.



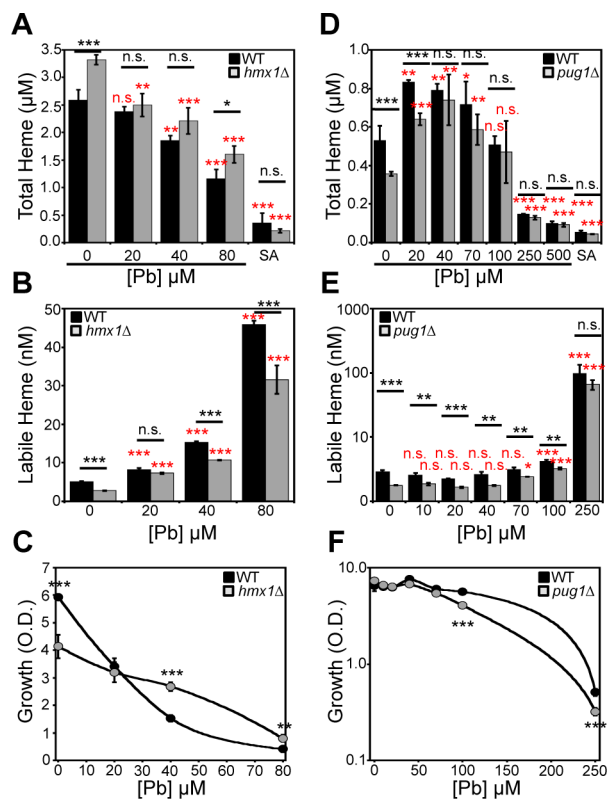


**Figure 6.**  $\text{Pb}^{2+}$ -induced depletion of heme is  $\text{O}_2$ -dependent. Cells expressing HS1-M7A were conditioned with the indicated concentration of  $\text{Pb}^{2+}$  and allowed to recover in an anoxic, nitrogen-rich ( $\text{N}_2$ ) atmosphere or in air ( $\text{O}_2$ ) and (A) total heme, (B) labile heme, and (C) viability were measured. All data represent the mean  $\pm$  SD of triplicate cultures and statistical significance was assessed using a two-sample t-test. Black asterisks represent the statistical significance between the indicated pairwise comparisons of conditions and red asterisks represent the statistical significance relative to 0  $\mu\text{M}$  [Pb]. \*  $P < 0.05$ , \*\*  $P < 0.01$ , \*\*\*  $P < 0.001$ , n.s. not significant.

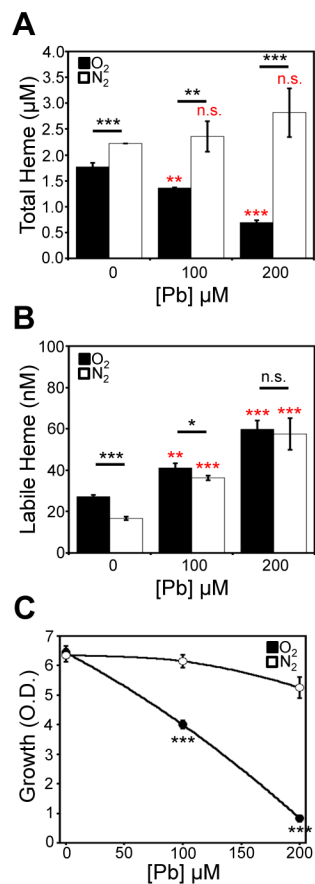


**Figure 7.** Pb<sup>2+</sup>-induced depletion of heme does not involve *HMX1* or *PUG1*. **(A-C)** *hmx1* $\Delta$  cells exhibit a Pb<sup>2+</sup>-dependent **(A)** decrease in total heme and **(B)** increase in labile heme. **(C)** *hmx1* $\Delta$  cells are more resistant to Pb<sup>2+</sup> toxicity. **(D-F)** *pug1* $\Delta$  cells exhibit a Pb<sup>2+</sup>-dependent **(D)** decrease in total heme, **(E)** increase in labile heme, and **(F)** WT-sensitivity to Pb<sup>2+</sup> toxicity. All data represent the mean  $\pm$  SD of triplicate cultures and statistical significance was assessed using a two-sample t-test. Black asterisks represent the statistical significance between the indicated pairwise comparisons of conditions and red asterisks represent the statistical significance relative to 0  $\mu$ M [Pb]. \* P < 0.05, \*\* P < 0.01, \*\*\* P < 0.001, n.s. not significant.

**Figure 8.**  $\text{Pb}^{2+}$ -dependent changes in heme homeostasis correlate with the degradation of a large fraction of the proteome and are affected by the proteasome. **(A)** SDS-PAGE and Coomassie staining of lysates prepared from cells conditioned with or without an  $\text{LD}_{50}$  dose of  $\text{Pb}^{2+}$ , 100  $\mu\text{M}$ , that did or did not undergo a post- $\text{Pb}^{2+}$  exposure recovery period. Tandem mass spectrometry reveals that the high intensity chromatic bands that are retained under  $\text{Pb}^{2+}$ -stress, indicated by the arrows, are GAPDH and enolase (**Table S2**). **(B)** The expression and activity of the high affinity hemoprotein Ctt1p, a heme-catalase enzyme, is down-regulated in response to  $\text{Pb}^{2+}$  conditioning, whereas GAPDH expression, a constituent of the labile heme buffer, is maintained. All gels are representative of at least three independent cultures. **(C and D)** The effects of *atg1Δ* (**C**), *rpn10Δ* (**C**), and *pep4Δ* (**D**) deletion on  $\text{Pb}^{2+}$ -dependent changes in labile heme were assessed. **(E and F)**  $\text{Pb}^{2+}$ -dependent changes in total heme (**E**) and growth (**F**) were assessed in WT and *rpn10Δ* cells. All labile and total heme measurements represent the mean  $\pm$  SD of triplicate cultures, whereas the growth data represent the mean  $\pm$  SD of duplicate cultures. Statistical significance was assessed using a two-sample t-test. Black asterisks represent the statistical significance between the indicated pairwise comparisons of conditions and red asterisks represent the statistical significance relative to 0  $\mu\text{M}$  [Pb]. \*  $P < 0.05$ , \*\*  $P < 0.01$ , \*\*\*  $P < 0.001$ , n.s. not significant, n.d. not detectable.

## **Heme bioavailability and signaling in response to stress in yeast cells**

David A. Hanna, Rebecca Hu, Hyojung Kim, Osiris Martinez-Guzman, Matthew P. Torres  
and Amit R. Reddi

*J. Biol. Chem.* published online June 19, 2018

---

Access the most updated version of this article at doi: [10.1074/jbc.RA118.002125](https://doi.org/10.1074/jbc.RA118.002125)

### Alerts:

- [When this article is cited](#)
- [When a correction for this article is posted](#)

[Click here](#) to choose from all of JBC's e-mail alerts